Heliyon 9 (2023) e15148

Contents lists available at ScienceDirect

Heliyon

journal homepage: www.cell.com/heliyon

Research article

Theoretical and numerical study of contaminant transport in clayey barriers using a revised numerical model considering the dependency of membrane efficiency and hydraulic conductivity on solute concentration

Hamed Sadeghi [*], Aysa Hedayati-Azar [1]

Department of Civil Engineering, Sharif University of Technology, Azadi Ave., Tehran, Iran

ARTICLE INFO

Keywords:
Soluble contaminants transport
Membrane efficiency
Hydraulic conductivity
Diffusion
Numerical simulation
Clayey barrier

ABSTRACT

Solid waste is often buried in landfills isolated with a bentonite-based clay barrier to guarantee the high quality of groundwater. As the efficiency of clay barriers is highly dependent on solute concentration, this study aims to modify membrane efficiency, effective diffusion, and hydraulic conductivity of bentonite-based clayey barriers exposed to saline environments for numerical investigation of solute transport in such barriers. Therefore, the theoretical equations were modified as a function of solute concentration instead of constant values. First, a model was extended for membrane efficiency as a function of void ratio and solute concentration. Second, an apparent tortuosity model was developed as a function of porosity and membrane efficiency to adjust the effective diffusion coefficient. Moreover, a recently developed semi-empirical solute-dependent hydraulic conductivity model was employed, which is dependent on solute concentration, liquid limit, and void ratio of the clayey barrier. Afterward, four approaches for applying these coefficients were defined as either "variable" or "constant" functions in ten numerical scenarios using COMSOL Multiphysics. The results reveal that "variable" membrane efficiency affects the outcomes in lower concentrations, while "variable" hydraulic conductivity is more influential in the domain of higher concentrations. Although all approaches converge to the same ultimate distribution of solute concentration using the Neumann exit boundary condition, the choice of different approaches clearly affects the ultimate state for the Dirichlet exit boundary condition. As the thickness of the barrier increases, the ultimate state is reached later, and choosing the approach to apply coefficients is more influential. Decreasing the hydraulic gradient postpones the solute breakthrough in the barrier, and picking the variable coefficients is more crucial in higher hydraulic gradients.

1. Introduction

One of the most popular means of waste management is the burial of waste in landfills and using clayey barriers under them to

* Corresponding author.
E-mail addresses: hsadeghi@sharif.edu (H. Sadeghi), aysa.hedayati9776@sharif.edu (A. Hedayati-Azar).
[1] Present Address: Department of Civil Engineering, Macdonald Engineering Building, McGill University, 817 Rue Sherbrook O #492, Montréal, Canada.

https://doi.org/10.1016/j.heliyon.2023.e15148
Received 7 January 2023; Received in revised form 27 March 2023; Accepted 28 March 2023
Available online 20 April 2023

prevent leachate leakage into the groundwater due to their low hydraulic conductivity and semipermeable behavior [1–4]. It was assumed that the possibility of groundwater and soil contamination is low in landfills with deep groundwater tables (i.e., natural loess) [5,6], whereas when the water table rises and reaches close to the landfill, the possibility of groundwater contamination increases. Therefore, it is even more substantial to explore the leachate leakage in saturated isolation barriers.

Bentonite-based clays are the preferable material for landfills, which are physiochemically active materials due to their intrinsic surface electrical charge, solid skeleton fabric, diffuse double layers [7–9]. When designing isolation clay barriers, salt should be considered as one of the indispensable contaminants in landfills [10,11].

Coupled hydro-chemical processes lead to contaminant transport and fluid flow in clayey barriers. Darcian and chemico-osmosis fluid flow are responsible for fluid transport, and contaminants are transported due to diffusion and convection [12]. Membrane efficiency, diffusion coefficient, and hydraulic conductivity are phenomenological coefficients affecting the transport process. Experimental results have revealed that these coefficients are extensively dependent on the solute concentration in the pore fluid [13–16]. However, these phenomenological coefficients were assumed to be constant in previous numerical studies regardless of the solute concentration of pore fluid, which is a fundamental limitation [17–20].

This paper aims to explore solute transport in clay barriers considering phenomenological coefficients as variables instead of constants using numerical methods in COMSOL Multiphysics. First, effective diffusion, membrane efficiency, and hydraulic conductivity coefficients are investigated as a function of solute concentration. Then, they are applied in various numerical scenarios to explore concentration-dependent coefficients on results.

2. Coupled hydro-chemical multiphase flow in clay barriers

A combination of both direct and coupled processes leads to fluid flow and solute transport in the porous medium of soil [4,12]. This paper focuses on the coupled hydro-chemico processes in chemically active clayey barriers. Direct conduction processes (i.e., hydraulic conduction based on Darcy's law and diffusion based on Fick's law) relate the flow directly to their driving gradients. Nevertheless, coupled conduction processes (i.e., chemico-osmosis fluid flow and convection) relate the flow of one type to the driving gradient of another kind [3,21]. In all of these processes, there are some phenomenological coefficients relating the fluid flow to the driving gradients, which play a crucial role in the transport process. Two types of driving gradients exist in clayey barriers in the landfill, which are responsible for solute transport in the barrier, including the hydraulic gradient due to the produced leachate in the landfill and the concentration gradient due to the presence of contaminants in the leachate. In the following sections, each process and its role in the clayey barrier will be investigated. Next, partial differential equations are presented to describe coupled multiphase flows in clayey barriers considering all of those processes.

2.1. Hydraulic conduction

Based on Darcy's law, hydraulic conduction happens due to the hydraulic gradient from the side with a higher hydraulic head to the side with a lower hydraulic head using Eq. (1) as follows [22–24]:

$$q_h = -k_h i_h = -k_h \frac{\partial h}{\partial y} \tag{1}$$

where, q_h is Darcian fluid flow, k_h is hydraulic conductivity (see section 4.1), i_h is hydraulic gradient, and h is hydraulic potential. The dependency of hydraulic conductivity on void ratio and subsequent changes in void ratio due to the hydration of clay minerals is well documented by experimental measurements [24]. In addition to the hydraulic gradient, the concentration gradient can also induce fluid flow in clayey barriers with semi-permeable behavior, which is explored in the following section.

2.2. Chemico-osmosis fluid flow and semipermeable behavior

Chemically active clayey soils, such as bentonite-based clay barriers, contain montmorillonite minerals. They absorb cations and water molecules, resulting in a layer of water and cations around them, known as the diffuse double layer. It makes clays chemically active and induces specific behaviors in them, such as very low hydraulic conductivity and a restrictive behavior against particle transport. The restriction ability of clays against solute transport is quantified by membrane efficiency (ω), which is ranged between 0 and 1 (see section 4.3). When membrane efficiency is equal to 0, there is no restriction against solute transport, while when it is equal to 1, solutes cannot move through the porous medium [25,26]. In the presence of solutes in the pore fluid, the diffuse double layer shrinks, and the clay's macropore ratio increases, which is followed by increased hydraulic conductivity and decreased membrane efficiency. It has also been proven experimentally [11,27–32].

Furthermore, semipermeable behavior also leads to chemico-osmosis fluid flow as a result of solute concentration gradients from the more diluted area to the more concentrated area, which is expressed by Eq. (2) as follows [19,26,32,33]:

$$q_\pi = k_\pi \frac{\partial \pi}{\partial y} = \frac{\omega k_h}{\gamma_w} \frac{\partial \Pi}{\partial y} = \frac{\omega k_h RT}{\gamma_w} \sum_{i=1}^{M} \frac{\partial C_i}{\partial y} \tag{2}$$

In this equation, q_π is chemico-osmosis fluid flow, k_π is chemico-osmosis conductivity, γ_w is unit weight of water, Π is chemico-osmosis potential based on Van 't Hoff equation, C_i is ion concentration, R is universal gas constant (8.314J/mol/K), T is absolute

temperature (K), and M is number of ions in the pore water [34].

Besides the chemico-osmosis fluid flow, the concentration gradient also induces diffusion of solutes in the porous media, which is discussed in the following section.

2.3. Diffusion

Solute moves through the porous media due to the concentration gradient from the concentrated area to the diluted area based on Fick's law using Eq. (3) as follows [35,36]:

$$J_d = -D_s^* \theta \frac{\partial c_s}{\partial y} = -D_0 \tau_a \theta \frac{\partial c_s}{\partial y} \tag{3}$$

In which θ is expressed by Eq. (4) as follows:

$$\theta = nS_r \tag{4}$$

$$\tau_a = \tau_m \tau_r \tag{5}$$

In this equation, J_d is diffusion flux, D_0 is diffusion coefficient in water, D_s^* is the effective diffusion coefficient, τ_a apparent is tortuosity factor, n is porosity, S_r is saturation degree, and c_s is salt concentration. τ_a is an essential factor that shows the effect of porous structure on the diffusion coefficient. It consists of two factors, including matrix tortuosity (τ_m) and restrictive tortuosity (τ_r). Matrix tortuosity adjusts the diffusion coefficient to consider the effect of porous media on lengthening the rout of particles in soil. Restrictive tortuosity initiates the impacts of membrane behavior of clays in the effective diffusion factor [8,35,37–39]. Eqs. (6) and (7) were suggested for these factors as follows [40–42]:

$$\tau_r = 1 - \omega \tag{6}$$

$$\tau_m = n^m \tag{7}$$

In these equations, m is an empirical factor.

2.4. Convection

Besides the diffusion, solutes also move as a result of fluid flow in the porous medium. Since two kinds of fluid flow (Darcian fluid flow and chemico-osmosis fluid flow) are considered in this study, the convection of solute also has two terms. Semipermeable behavior also affects solute convective flow. As a result, Eq. (8) was proposed for the convection of solutes [19,43]:

$$J_A = J_{a,h} + J_{a,\pi} = (1-\omega) c_s (q_h + q_\pi) = (1-\omega) c_s k_h \left(\frac{\omega}{\gamma_w} \frac{\partial \Pi}{\partial y} - \frac{\partial h}{\partial y} \right) \tag{8}$$

2.5. Partial differential equations of coupled multiphase flow

In order to develop governing partial differential equations for fluid flow and solute transport in a clayey barrier, all the above-mentioned processes are considered. The following equations were driven assuming infinitely diluted solution, isothermal condition, no electric charge, saturated soil condition, one-dimensional flow, solid skeleton, incompressible fluid, no soil deformation, and conservation of mass [19]:

$$\frac{\partial q}{\partial y} = \frac{\partial}{\partial y} \left[-k_h \frac{\partial h}{\partial y} + k_h \frac{\omega RT}{\gamma_w} \sum_{i=1}^{M} \frac{\partial C_i}{\partial y} \right] = 0 \tag{9}$$

$$R_d n \frac{\partial c_s}{\partial t} = -\frac{\partial}{\partial y} \left[(1-\omega) q_h c_s + (1-\omega) q_\pi c_s - n D_0 (1-\omega) \tau_m \frac{\partial c_s}{\partial y} \right] = 0 \tag{10}$$

In this equation, R_d is the retardation factor, expressing the adsorbed part of solutes [19]. Eq. (9) and Eq. (10) are used for in the numerical modelling of solute transport in clayey barriers.

The presence of $(1-\omega)$ in all terms on the right-hand side of Eq. (10) demonstrates the inhibitory role of membrane behavior of clayey soils on solute transport. When the barrier acts as an ideal semi-permeable membrane, solutes are able to be transported through neither the convection nor the diffusion fluxes.

3. Material

The first step of numerical analysis is to determine the material. As bentonite is a chemically active soil with intense membrane behavior and high sensitivity to the presence of solutes in the pore water, bentonite-based clays were chosen in this study. As this study intends to simulate the solute transport in a clayey barrier using solute-dependent empirical or semi-empirical coefficients, picking the material should be based on the availability of existing experimental data on the various material. Exploring experimental results

reveals that the number of data points on membrane efficiency and diffusion coefficient of bentonite in Bentomat® geosynthetic clay liners is more compared with other bentonite material. Characteristics of this material and its existing data sets are mentioned respectively in Table 1 and Table 2.

4. Phenomenological coefficients

According to Eq. (9) and Eq. (10), phenomenological coefficients (membrane efficiency, hydraulic conductivity, and apparent tortuosity) play a significant role in the governing equations of solute transport. These coefficients and their dependency on solute concentration are discussed in the following sections.

4.1. Hydraulic conductivity

Hydraulic conductivity increases by increasing solute concentration in the pore fluid due to the effect of solutes on the thickness of the diffuse double layer, which is also admitted by experimental results. Besides that, hydraulic conductivity directly affects the Darcian fluid flow, chemico-osmosis fluid flow, and solute transportation by convection [15,45–47]. Following equation was suggested to quantify the hydraulic conductivity as a function of solute concentration in bentonite-based clays [30]:

$$k_h(\mathrm{cm/s}) = 6.992\frac{\gamma_w}{\mu_w}\frac{1}{\rho_s^2}\frac{e^{0.625}}{1+e}\frac{1}{w_{Lc}^{2.039+0.947/e}} \tag{11}$$

$$w_{Lc} = w_{L0} - \left(\frac{89.460}{1+\exp(2.595-0.007\times w_{L0})} - 7.152\right) ln(1+c_s) \tag{12}$$

Chapuis (2012) reviewed various models for hydraulic conductivity of two types of plastic and non-plastic soils [48]. Based on the results, Mbonimpa et al.'s model (2002) [49] has the best performance compared with other models of plastic soils. This model was developed for hydraulic conductivity as a function of solute concentration using the previous model of Mbonimpa et al. (2002) for hydraulic conductivity of deionized water. Mbonimpa et al.'s model (2002) is based on the well-known model of Kozeny-Carman adjusted for plastic soils [49–51]. Hedayati-Azar and Sadeghi (2022) modified the coefficients and powers of Mbonimpa et al.'s hydraulic conductivity model (2002) in Eq. (12), and proposed a liquid limit model to reflect its dependency on solute concentration [30].

4.2. Apparent tortuosity

Apparent tortuosity is a function of membrane efficiency and porous structure characteristics and modifies the diffusion coefficient. As was mentioned in Eq. (5), apparent tortuosity is formed out of two terms including matrix tortuosity and restrictive tortuosity. Employing the previously-developed models (i.e., Eq. (7)) leads to an inaccurate anticipation of apparent tortuosity of data sets reported in Table 2. Therefore, a new model should be developed for apparent tortuosity for the purpose of this study. In this regard, the following equation is proposed:

$$\tau = an^m(1-\omega) \tag{13}$$

Correlating data sets reported in Table 2 with Eq. (13) leads to the following constants with the coefficient of determination equal to.

$$\tau = \tau_m\tau_r = 0.177n^{2.004}(1-\omega) \tag{14}$$

Fig. 1 shows the apparent tortuosity as function of membrane efficacy and porosity. Although the coefficient of determination is still low, it is practical enough for this study. The low coefficient of determination of this model is due to several factors, including different methods for measuring diffusion coefficient, the transient flux of diffusion in the initial stages of measuring, the adsorption of cations to a clay matrix, the correlation between restriction ability and matrix tortuosity, etc. [39,42,52].

Table 1
Assumptions regarding the materials used in the models.

Parameter	Amount
Soil type	Na bentonite
Contaminant type	KCl
Initial condition	$c_s(y,t=0) = 0$
Specific gravity, G_s	2.43
Liquid limit, LL(%)	478
Plastic index, PI(%)	439
Water unit weight, γ (kN/m^3)	9.8
Retardation factor, R_d	1
Absolute temperature, T (K)	298
Void ratio, e	3

Table 2
Summary of experimental data sets used for developing empirical and semi-empirical models.

Reference	Type of apparatus	No. of data points for membrane efficiency	No. of data points for diffusion
Malusis & Shackelford (2002b) [32]	Rigid wall	14	4
Kang & Shackelford (2009) [14]	Flexible wall	9	0
Kang & Shackelford (2011) [44]	Flexible wall	20	20
Shackelford et al. (2016) [42]	Rigid wall	6	6

4.3. Membrane efficiency

A clayey barrier's membrane efficiency is crucial for solute transport because it directly affects all processes (convection and diffusion fluxes) as shown in Eq. (10). Experimental results also demonstrate that the membrane efficiency decreases by increasing concentration due to the shrinkage of diffuse double layer. Since membrane efficacy directly affects the chemico-osmosis fluid flow, convection, and diffusion, its crucial role in results cannot be denied [13,19,53–56]. The physical approach on the microscopic scale proposes a model for membrane efficiency of bentonite soils using monovalent salts using Eq. (15) as follows [27,28]:

$$\omega = 1 - \frac{1}{\sqrt{\left(\frac{\overline{c'}_{sk,0}}{2c_s e}\right)^2 + 1 + (2t_c - 1)\left(\frac{\overline{c'}_{sk,0}}{2c_s e}\right)}} \tag{15}$$

In which t_c is expressed by Eq. (16) as follows:

$$t_c = \frac{D_{oc}}{D_{oc} + D_{oa}} \tag{16}$$

In this equation, $\overline{c'}_{sk,0}$ is solid skeleton charge concentration, D_{oc} is diffusion coefficient of cation, and D_{oa} is diffusion coefficient of anion.

The experimental procedure for measuring membrane efficiency is applied on a very thin layer of clay. As membrane efficiency is a function of solute concentration, it is not constant all over the clayey barrier. Having assumed a linear distribution of solute in the clayey layer, Eq. (17) is derived as follows [27,28,33,57]:

$$\omega_g = 1 + \frac{\overline{c'}_{sk,0}}{2e\Delta c_s}\left[Z_2 - Z_1 - (2t_c - 1)ln\left(\frac{Z_2 + 2t_c - 1}{Z_1 + 2t_c - 1}\right)\right] \tag{17}$$

In which Z_1 is expressed by Eq. (18) as follows:

$$Z_1 = \sqrt{1 + \left(\frac{2C_t e}{\overline{c'}_{sk,0}}\right)^2} \tag{18}$$

And Z_2 is expressed by Eq. (19) as follows:

$$Z_2 = \sqrt{1 + \left(\frac{2C_b e}{\overline{c'}_{sk,0}}\right)^2} \tag{19}$$

In this equation, C_t is the solute concentration at the top boundary of the soil, C_b is the solute concentration at the bottom boundary.

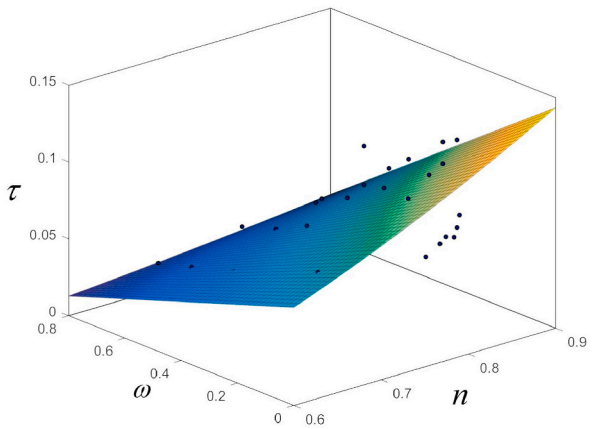

Fig. 1. Tortuosity versus membrane efficiency and porosity.

In these equations, the amount of $\overline{c'}_{sk,0}$ is not determined. However, it is known that its value is dependent on the void ratio and solute concentration [7,9]. Based on data sets on membrane efficiency, Eq. (20) is proposed for $\overline{c'}_{sk,0}$ as follows:

$$\overline{c'}_{sk,0} = \frac{e^{p_e}(0.5(C_t + C_b))^{p_c}}{a_s} \tag{20}$$

Correlating the data sets reported in Table 2 with the abovementioned equation leads to Eq. (21) with the coefficient of determination equal to 0.854 as follows:

$$\overline{c'}_{sk,0} = \frac{e^{0.731}(0.5(C_t + C_b))^{0.125}}{38.615} \tag{21}$$

Although various methods were used to measure the membrane efficiency data sets reported in Table 2, the coefficient of determination shows adequate compatibility between data sets and the proposed model. Consequently, the following equation is derived for membrane efficiency as a function of void ratio and solute concentration:

$$\omega = 1 - \frac{1}{\sqrt{\left(\frac{1}{77.230 c_s^{0.875} e^{0.269}}\right)^2 + 1} - 0.0175\left(\frac{1}{77.230 c_s^{0.875} e^{0.269}}\right)} \tag{22}$$

This section discussed practical models for hydraulic conductivity, effective diffusion coefficient (or apparent tortuosity), and membrane efficiency only as a function of solute concentration, void ratio, and liquid limit. Accordingly, Eqs. (11), (14) and (22) can be used in Eqs. (9) and (10) to simulate coupled hydro-chemical fluid flow and solute transport in a clayey barrier.

5. Research methodology

Previous numerical studies on coupled hydro-chemical fluid flow and solute transport assumed the constant amounts of hydraulic conductivity and membrane efficiency in the clayey barrier during the time, which was a serious limitation [17–20]. In another study, it was assumed that membrane efficacy is a variable, while hydraulic conductivity is still assumed to be a constant value [58].

This study provides semi-empirical and empirical models for hydraulic conductivity, effective diffusion coefficient, and membrane efficiency. Hence, these phenomenological coefficients can be used in a numerical model to simulate the transport of solutes in a bentonite-based clay barrier considering their dependency on solute concentration. In order to investigate the deviation of results after applying variable coefficients, four approaches are defined in Table 3. This study takes various solute concentrations, exit boundary conditions, barrier thicknesses, and hydraulic gradients into consideration, which are stated in Table 4.

As mentioned, solute transport deals with coupled processes in the porous media. In this regard, COMSOL Multiphysics is a perfect choice as it is a very strong numerical software for modelling coupled processes. In addition, it has developed packages for modelling solute transport and fluid flow [59].

A schematic Figure of the bentonite-based clay barrier is demonstrated in Fig. 2. It is assumed that the leachate, which contains solute particles, is located at the top boundary of the isolation clayey barrier, and the system is fully saturated [60]. Therefore, the direction of chemico-osmosis fluid flow is from the exit boundary at the bottom of the layer to the entrance boundary. In addition, the direction of diffusion flux is from the entrance boundary to the exit boundary due to the higher solute concentration at the top boundary. The direction of Darcian fluid flow is from the entrance boundary to the exit boundary as well.

COMSOL Multiphysics' numerical model for coupled hydro-chemical flow governing the solute transport in clayey barriers is verified against previous numerical studies. However, as was mentioned, previous studies assumed constant values for both hydraulic conductivity and membrane efficiency. Table 5 shows the assumptions of Malusis and Shackelford's model (2004) [20] and Manassero and Dominijanni's model (2003) [19], which are demonstrated respectively by M&Sh and M&D labels in Fig. 3(a) and (b). This study applied their assumption in COMSOL Multiphysics to verify this study's model in this numerical software. As Fig. 3 demonstrates, the numerical results of previous studies and the results of this study using COMSOL Multiphysics are the same.

6. The interpretation of results

In order to investigate the differences between different approaches to applying hydraulic conductivity and membrane efficiency, outcomes of various numerical scenarios will be discussed and compared in this section.

Table 3
Introducing approaches for applying membrane efficiency and hydraulic conductivity.

Coefficient	Membrane Efficiency		Hydraulic Conductivity	
Approach	Constant	Variable	Constant	Variable
mc-kc	✔		✔	
mv-kc		✔	✔	
mc-kv	✔			✔
mv-kv		✔		✔

Table 4
Input parameters in the numerical scenarios.

Scenarios	Parameters	Amounts	Heading Numbers			
			C_0	EBC	L	i_h
1	Source solute concentration, C_0(mM)	5	6.1			
	Exit boundary condition, EBC	$\partial C(L,t)/\partial y = 0$		6.2		
	Thickness of barrier, L(m)	1				
	Hydraulic gradient, i_h	5				
2	Source solute concentration, C_0(mM)	50	6.1			
	Exit boundary condition, EBC	$\partial C(L,t)/\partial y = 0$		6.2		
	Thickness of barrier, L(m)	1			6.3	
	Hydraulic gradient, i_h	5				6.4
3	Source solute concentration, C_0(mM)	500	6.1			
	Exit boundary condition, EBC	$\partial C(L,t)/\partial y = 0$		6.2		
	Thickness of barrier, L(m)	1				
	Hydraulic gradient, i_h	5				
4	Source solute concentration, C_0(mM)	5				
	Exit boundary condition, EBC	$C(L,t) = 0$		6.2		
	Thickness of barrier, L(m)	1				
	Hydraulic gradient, i_h	5				
5	Source solute concentration, C_0(mM)	50				
	Exit boundary condition, EBC	$C(L,t) = 0$		6.2		
	Thickness of barrier, L(m)	1				
	Hydraulic gradient, i_h	5				
6	Source solute concentration, C_0(mM)	500				
	Exit boundary condition, EBC	$C(L,t) = 0$		6.2		
	Thickness of barrier, L(m)	1				
	Hydraulic gradient, i_h	5				
7	Source solute concentration, C_0(mM)	50				
	Exit boundary condition, EBC	$\partial C(L,t)/\partial y = 0$				
	Thickness of barrier, L(m)	0.5			6.3	
	Hydraulic gradient, i_h	5				
8	Source solute concentration, C_0(mM)	50				
	Exit boundary condition, EBC	$\partial C(L,t)/\partial y = 0$				
	Thickness of barrier, L(m)	2			6.3	
	Hydraulic gradient, i_h	5				
9	Source solute concentration, C_0(mM)	50				
	Exit boundary condition, EBC	$\partial C(L,t)/\partial y = 0$				
	Thickness of barrier, L(m)	1				
	Hydraulic gradient, i_h	1.1				6.4
10	Source solute concentration, C_0(mM)	50				
	Exit boundary condition, EBC	$\partial C(L,t)/\partial y = 0$				
	Thickness of barrier, L(m)	1				
	Hydraulic gradient, i_h	15				6.4

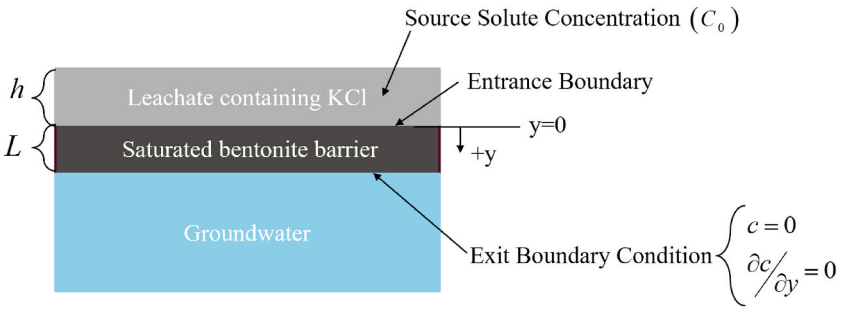

Fig. 2. Schematic bentonite-based clayey barrier and boundary conditions.

Fig. 4 shows the membrane efficiency profile in the first, tenth, and hundredth years using the four approaches from Table 3. As this Figure reveals, the constant membrane efficiency in mc-kc and mc-kv approaches is higher than the variable values in shallow depths of the barrier and is lower in the deeper parts in the early years. As a result, mc-kc and mc-kv approaches assume more restriction ability close to the entrance boundary and less restriction ability close to the exit boundary compared with mv-kc and mv-kv approaches.

Moreover, comparing Fig. 4(a), (b), and (c) reveals that the amount of membrane efficiency decreases during the time as solutes invade the exit boundary. Consequently, Fig. 4(c) shows that, finally, the amount of membrane efficiency would be almost constant in

Table 5
Input parameters for the verification of numerical model in COMSOL Multiphysics.

Reference	M&Sh (Malusis and Shackelford (2004) [20])	M&D (Manassero and Dominijanni (2003) [19])
Source concentration, C_0 (mM)	8.7	5.0
Barrier thickness, L(m)	1.00	0.01
Hydraulic gradient, i_h	10	10
Exit boundary condition, EBC	$c_s(L,t) = 0$	$\partial c_s(L,t)/\partial y = 0$
Initial solute Concentration, c_s (mM)	$c_s(y,t=0) = 0$	$c_s(y,t=0) = 0$
Porosity, n	0.79	0.70
Temperature, T(K)	298	293
Hydraulic conductivity, k_h(m/s)	1.33×10^{-10}	1.00×10^{-10}
Membrane efficiency, ω	0.0 (NM, I), 0.49 (E, EI)	0.0, 0.2, 0.4, 0.6, 0.8
Diffusion Coefficient, D_j^* (m^2/s)	$19.93 \times 10^{-10} \times 0.12$ (NM, E), $19.93 \times 10^{-10} \times 0.063$ (I, EI)	2×10^{-10}

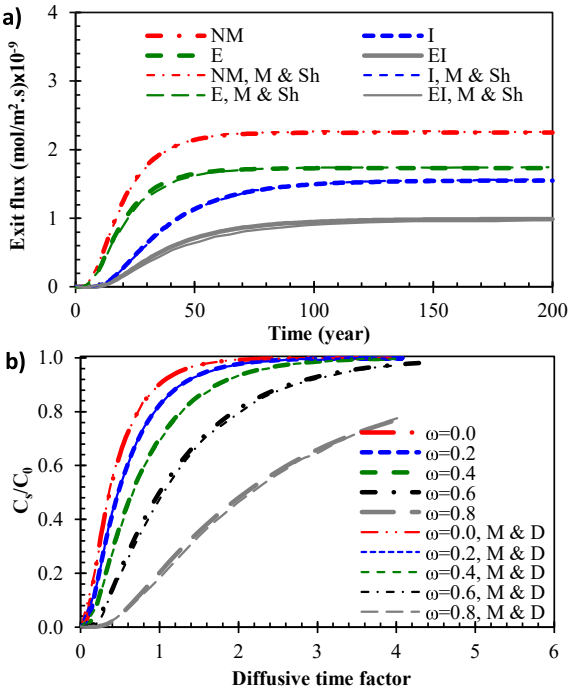

Fig. 3. Solute transport results in the clayey barrier using the numerical method in COMSOL Multiphysics and results of a) Malusis and Shackelford's (2004) study [20] and b) Manassero and Dominijanni's (2003) study [19] using input parameters in Table 5.

the barrier, and its amount is lower than the constant values in mc-kc and mc-kv approaches. It implies that using the constant membrane efficiency leads to more restriction ability in the long term since the constant approach proposes an average value based on the linear distribution of solutes in the barrier, while the solute distribution goes beyond the linear distribution over time.

Fig. 5 shows the hydraulic conductivity profile using the four approaches stated in Table 3. The constant hydraulic conductivity assumes the hydraulic conductivity of the clay barrier to be the same for both DI water and solution as the pore fluid. Accordingly, its values in mc-kc and mv-kv approaches are lower than its values in variable hydraulic conductivity (mc-kv and mv-kv) in all scenarios. Moreover, as solute concentration is higher in the shallower parts of the barrier in the early years, the hydraulic conductivity is also higher in shallower parts of the barrier. Comparing Fig. 5(a), (b), and (c) indicate that by breakthrough of solute to the deeper parts over time, hydraulic conductivity increases. Therefore, the fluxes of convection and Darcian fluid flow increase due to the effect of solute on hydraulic conductivity. Besides the hydraulic conductivity, chemico-osmosis fluid flow is also dependent on membrane efficiency.

Fig. 6(a), (b), and (c) show the solute concentration profile using all four approaches discussed in Table 3, respectively, in the first, tenth, and hundredth years. Based on this Figure, the solute concentration profile is relatively the same for all the four approaches in the first year because the effect of variable approaches is limited to shallower parts of the clayey barrier in the early years. However, the difference between different approaches becomes more evident over time. This Figure asserts that in the long term, the rate of solute transportation is the highest using the mv-kv approach, while it is the least when applying the mc-kc approach using the assumptions of scenario 2.

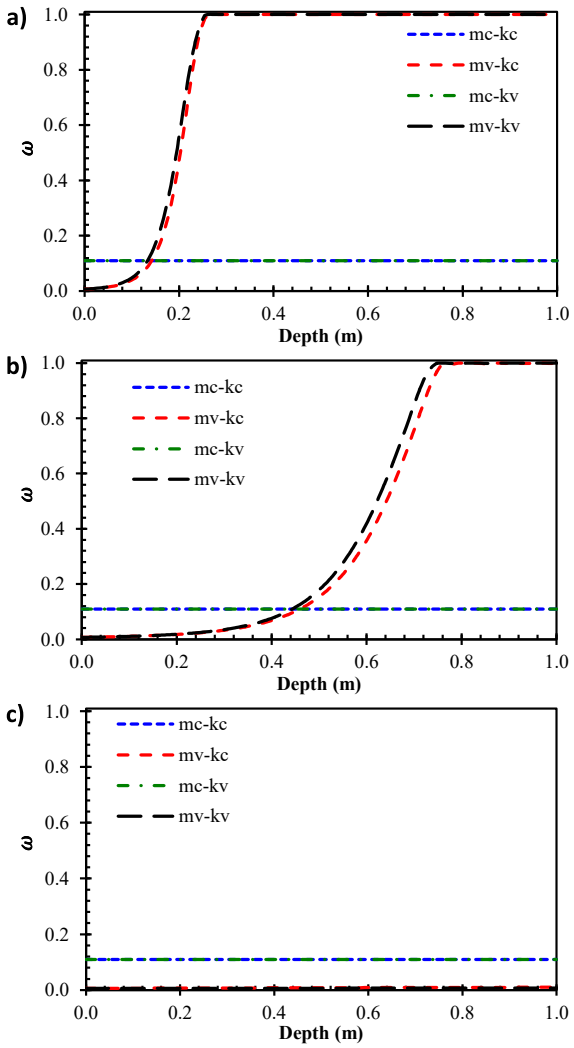

Fig. 4. Membrane efficiency profile at a) 1st year, b) 10th year, and c) 100th year in Scenario 2 in Table 4.

The results of this section were provided based on the assumptions of scenario 2, while by changing some assumptions, the results may also change. Hence, to reach an extensible conclusion about the effect of choosing approaches for applying hydraulic conductivity and membrane efficiency, various scenarios are selected. In this study, the importance of various parameters including source solute concentration, exit boundary condition, the thickness of barrier, and hydraulic gradient is explored and discussed. The specific condition of each variable is summarized in Table 4 for various numerical scenarios.

6.1. Source solute concentration

In order to explore the effect of source solute concentration at the entrance boundary on the results using the four approaches (based on Table 3), scenarios 1, 2, and 3 were defined as it is described in Table 4. Fig. 7 shows the breakthrough of solute concentration at the exit boundary during the time for these three scenarios.

First, the rate of change is lower when the source solute concentration is more dilute as the membrane efficiency is higher, which results in more restriction toward solute transport in the clayey barrier. Fig. 7(a) shows that the solute breakthrough in the exit boundary is slower when using the mv-kc and mv-kv approaches since there is higher membrane efficiency in the deeper parts of the barrier. However, reaching solute to the deeper parts leads to lower membrane efficiency in mv-kc and mv-kv over time. Consequently, the solute concentration becomes more at the exit boundary of the barrier in the long term by using the mv-kc and mv-kv approaches. As shown in Fig. 7(a), (b), and (c), solutes require less time in more concentrated areas to reach the exit boundary in the mc-kc and mc-kv approaches than do less concentrated areas.

Comparing mc-kv and mv-kv approaches in Fig. 6(c) demonstrates that the choosing approach for applying membrane efficiency also affects the result even when membrane efficiency is extremely low. Although the membrane efficiency is low in this case, the

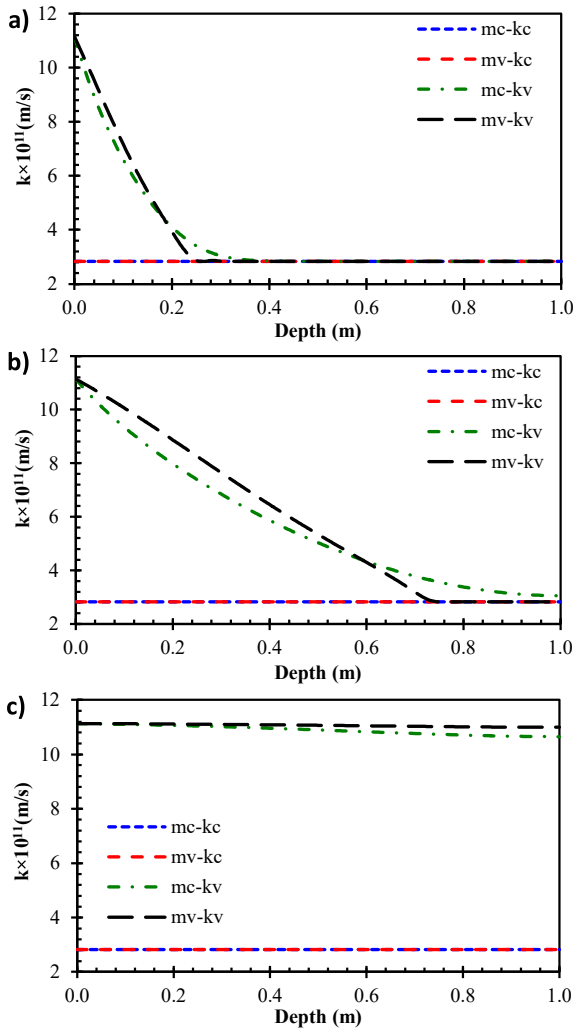

Fig. 5. Hydraulic conductivity profile at a) 1st year, b) 10th year, and c) 100th year in Scenario 2 in Table 4.

difference between applying the membrane efficiency as a variable or constant is significant due to the high hydraulic conductivity value, which leads to higher chemico-osmosis fluid flow as well. Eventually, because membrane efficiency is lower in the mv-kv approach than in the mc-kv approach, the chemico-osmosis fluid flow acts as a damper of Darcian fluid flow in the convection, which results in a slower breakthrough of solutes at the exit boundary.

Furthermore, Fig. 7 indicates that the difference between the four approaches is more perceptible when the source solute concentration is higher. In particular, higher solute concentrations lead to higher hydraulic conductivity values as well. Therefore, although the difference between mc-kc and mv-kc approaches and mc-kv and mv-kv approaches are noticeable in higher source solute concentrations (Fig. 7(c)), it is ignorable for dilute source solute concentrations (Fig. 7(a)).

Figs. 8 and 9 show the solute concentration profile respectively at the tenth- and hundredth-years using scenarios 1, 2, and 3. It indicates that using the variable hydraulic conductivity makes a negligible difference in the results of diluted concentrations, while the variable membrane efficiency alters the concentration profile evidently in this condition. As Fig. 8(a) shows solute concentration is lower in the shallower parts of the barrier when using the mc-kc and mc-kv approaches. Nevertheless, using the mv-kc and mv-kv approaches leads to lower concentrations in the deeper parts of the barrier in early years. Fig. 9(a) reveals that by increasing the solute concentration in the barrier, variable hydraulic conductivity increases, which is followed by a limited impact on the result in the dilute concentration in the long term.

Furthermore, Fig. 8(b) and (c) illustrate that the mc-kv approach provides relatively a lower solute concentration profile compared with other approaches using scenarios 2 and 3. It happens because of the effect of variable hydraulic conductivity on chemico-osmosis fluid flow and the inhibitory role of its convection, which results in a slower breakthrough of solutes in the barrier. However, solute concentration increases over time, which eventuates in higher hydraulic conductivity. Besides that, the concentration gradient decreases over time, which is followed by lower chemico-osmosis fluid flow and diffusion flux. Hence, the role of chemico-osmosis fluid flow in the convection flux becomes negligible eventually, which means a higher solute transport rate toward the exit boundary. In this

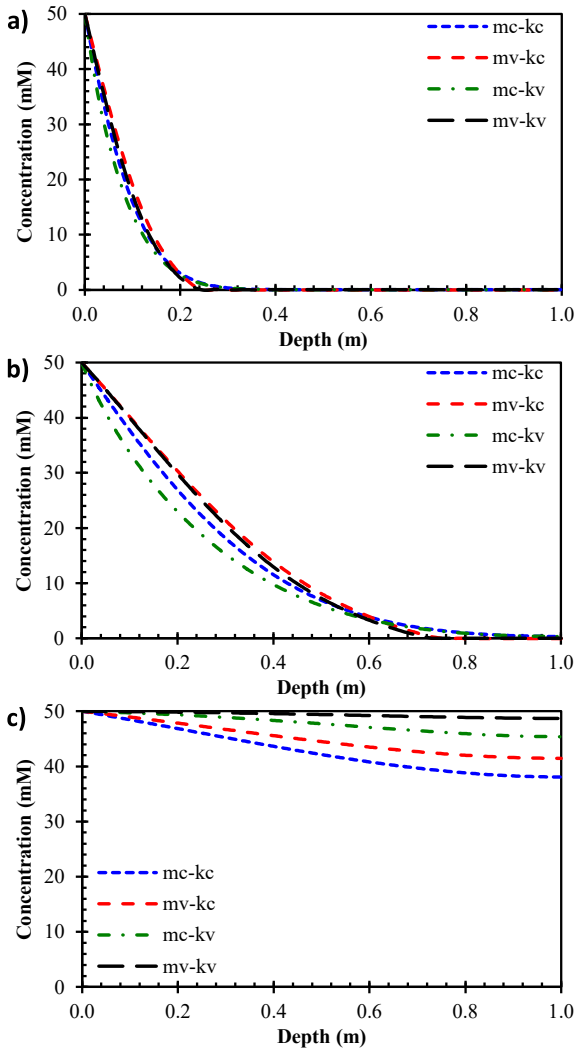

Fig. 6. Concentration profile at a) 1st year, b) 10th year, and c) 100th year in Scenario 2 in Table 4.

regard, Fig. 9 (b) and (c) also show higher solute concentration for the mc-kv approach compared with the mc-kc and mv-kc approaches.

Fig. 7 also shows a transient condition in early years. Eventually, a steady-state condition appears, and all the barrier is contaminated by the salt uniformly. At this point, the concentration gradient is eliminated, which means no diffusion flux and chemico-osmosis fluid flow. Therefore, hydraulic conductivity remains constant, which leads to a steady-state Darcian fluid flow and convection as it is reached for mc-kv and mv-kv condition in Figs. 7(c) and Fig. 9(c). The steady-state condition reaches faster when using variable approach for applying both hydraulic conductivity and membrane efficiency.

Scenarios 1, 2, and 3 assume the Neuman boundary condition governs the exit boundary, which results in a steady-state uniform solute distribution in the barrier. However, using a different boundary condition may alter the results. The following section examines the influence of boundary conditions on the results.

6.2. *Exit boundary condition*

In order to examine the effect of the exit boundary condition on the results of solute distribution and soluble contaminates breakthrough in the barrier, scenarios 4, 5, and 6 were defined with a different exit boundary condition compared to scenarios 1, 2, and 3 in Table 4. Figs. 10 and 11 show the average solute concentration breakthrough in the clayey barrier during the time using respectively $\partial c(L,t)/\partial y = 0$ and $c(L,t) = 0$ as the exit boundary condition.

First, it should be noted that the final steady-state condition differs between these two types of boundary conditions. Based on Fig. 10(c), the average solute concentration in the barrier is equal to the source solute concentration in the steady-state condition, while the average solute concentration is less than the source solute concentration when using $c(L,t) = 0$ as the exit boundary

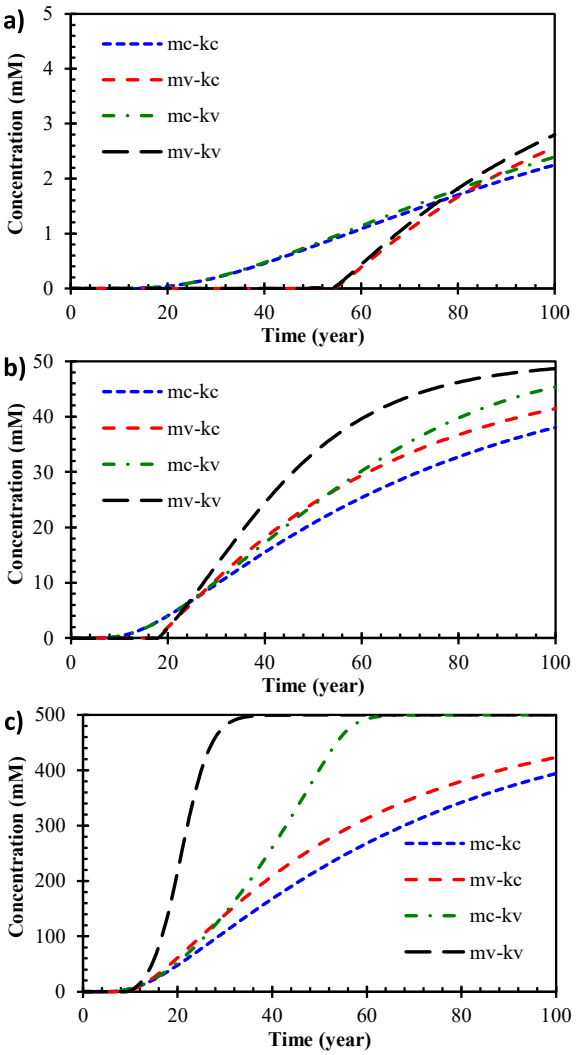

Fig. 7. Breakthrough of solute concentration at the exit boundary of the barrier in a) scenario 1, b) scenario 2, and c) scenario 3 in Table 4.

condition as it is indicated in Fig. 11(c). It happens because the exit boundary condition is imposed to have zero solute concentration. Moreover, the average solute concentration reaches the different ultimate values when using different approaches for applying membrane efficiency and hydraulic conductivity. Thus, the exit boundary condition plays a key role in the ultimate state of the barrier.

As both Figs. 10 and 11 show, the threshold values are reached during the 100 years when source solute concentration is high. However, Fig. 10(a) and (b) indicate that the final threshold value is not attained within 100 years due to the low initial solute concentration of the source. Furthermore, Fig. 11 demonstrates that the relative amount of threshold average solute concentration is higher when the source solute concentration is higher.

Additionally, Fig. 11 reveals the threshold solute concentration is the highest for mv-kv approach and lowest for mc-kc approach. However, a general conclusion cannot be made for mc-kv and mv-kc approaches since, depending on the source solute concentration, various results are obtained. Fig. 11(a), (b), and (c) demonstrates that the difference between the average solute concentration of mv-kv approach and other approaches increases by increasing source solute concentration.

Figs. 10 and 11 illustrate that although the exit boundary condition exerts a substantial influence on the final distribution of solutes in the barrier, it does not affect the distribution of solute concentrations in the early years. Thus, all explanations regarding scenarios 1, 2, and 3 (Fig. 8) also applies to scenarios 4, 5, and 6 in the early years.

Fig. 12 illustrates the solute concentration profiles in the barrier in the hundredth year. Comparing Fig. 9(a), (b), and (c) and Fig. 12 (a), (b), and (c) shows a faster breakthrough of solute transportation when using $\partial c(L,t)/\partial y = 0$ as the exit boundary condition due to the effect of strong membrane behavior close to the bottom of the barrier when using $c(L,t) = 0$. Using $c(L,t) = 0$ boundary condition also leads to lower hydraulic conductivity and higher solute concentration gradient close to the exit boundary. Higher concentration gradient and membrane efficiency lead to higher chemico-osmosis fluid flow and higher convection of chemico-osmosis fluid flow. Thus, comparing Fig. 9(b) and (c) with Fig. 12(b) and (c) demonstrates the slower breakthrough of solutes using $c(L,t) = 0$ as the exit

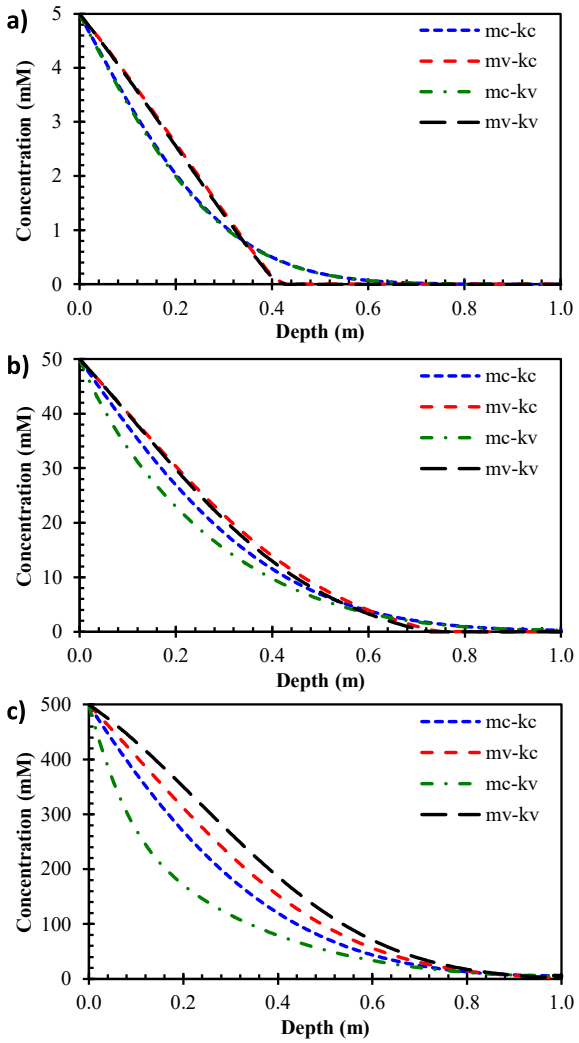

Fig. 8. Solute concentration profile in a) scenario 1, b) scenario 2, and c) Scenario 3 in Table 4 in the 10th year.

boundary condition instead of $\partial c(L,t)/\partial y = 0$, and the decrease is more significant when using the mc-kv approach compared with the mv-kc approach. In particular, mc-kv and mv-kc approaches result in relatively the same ultimate solute concentration profile in the barrier when using $c(L,t) = 0$ as the exit boundary condition, while using $\partial c(L,t)/\partial y = 0$ as the boundary condition leads to the higher solute profile in the mc-kv approach compared with the mv-kc approach.

It is also noteworthy that the variable hydraulic conductivity and membrane efficiency is followed by the lower membrane efficiency and higher hydraulic conductivity in the long term in all cases.

6.3. *Thickness of barrier*

In order to compare the results of variable and constant approaches for applying membrane efficiency and hydraulic conductivity in the previous sections, it was assumed that the thickness of clayey barrier is equal to 1 m. However, this section aims to explore the role of thickness of barrier on the result. Therefore, scenarios 7 and 8 are defined in Table 4 to be compared with scenario 2. Fig. 13 shows the average solute concentration breakthrough in the barrier using four approaches in Table 3. Fig. 13(a) shows a faster breakthrough when the layer is thinner as solutes reach the exit boundary faster. Accordingly, comparing Fig. 13(a), (b), and (c) indicates that the steady-state condition reaches faster thinner barriers.

In addition, Fig. 13 demonstrates that by increasing the thickness of the barrier, the difference between the ultimate average solute concentrations becomes more considerable in various approaches for applying membrane efficacy. Although the difference between the ultimate conditions of various approaches is more noticeable in thicker barriers in the long term, the difference is more significant in thinner barriers in the early years.

In scenarios 1 to 8, it was assumed the hydraulic gradient is equal to 5, while changing the hydraulic gradient also exerts influence

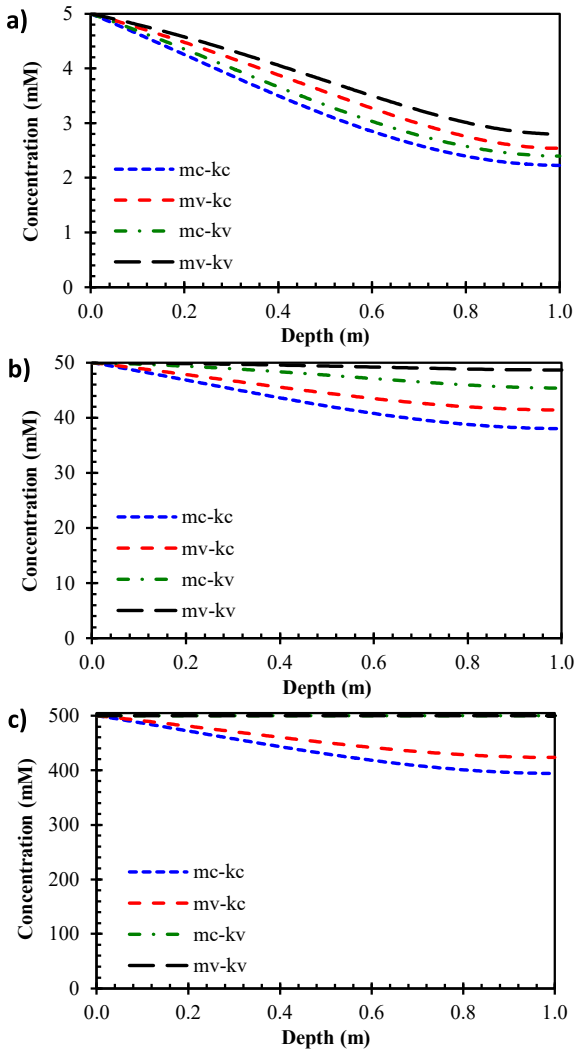

Fig. 9. Solute concentration profile in a) scenario 1, b) scenario 2, and c) Scenario 3 in Table 4 in the 100th year.

on the Darcian fluid flow and convection. The following section examines the influence of hydraulic gradients on the results.

6.4. Hydraulic gradient

Scenarios 9 and 10 were defined in Table 4 to explore the effect of hydraulic gradient on the results of solute distribution. The lower hydraulic conductivity leads to the lower Darcian fluid flow and, as a result, lower solute convection. Fig. 14 demonstrates the average solute concentration breakthrough in the barrier for scenarios 9, 2, and 10 using four different approaches based on Table 3. Comparing Fig. 14(a), (b), and (c) indicate a faster breakthrough of solute concentration in higher hydraulic gradient for all approaches.

First, Fig. 14(a) shows the result for the lowest hydraulic gradient. On the one hand, the Darcian fluid flow convection is negligible, which results in a negligible difference between the average solute concentration breakthrough of the mv-kc and mv-kv approaches. On the other hand, the chemico-osmosis fluid flow convection plays a more significant role compared to the Darcian fluid flow convection in low hydraulic gradients. Hence, Fig. 14(a) demonstrates that the mc-kv approach results in a slower breakthrough in comparison with the mc-kc approach. Therefore, in contrast with the average concentration breakthrough of mc-kv approach in scenario 10 with a higher hydraulic gradient (Fig. 14(c)), the average concentration breakthrough of the mc-kv approach in scenario 9 (Fig. 14(a)) never reaches the average concentration breakthrough of the mc-kc approach during the 100 years.

Fig. 14(a) also reveals a faster breakthrough of the solute concentration in the barrier when using the mv-kc approach in the early years since Darcian fluid flux convection is negligible due to the low hydraulic gradient, and constant hydraulic conductivity and variable membrane efficiency (mv-kc) lead to the low chemic-osmosis fluid flux convection. Variable hydraulic conductivity results in higher chemic-osmosis fluid flux convection toward the entrance boundary in lower hydraulic gradients.

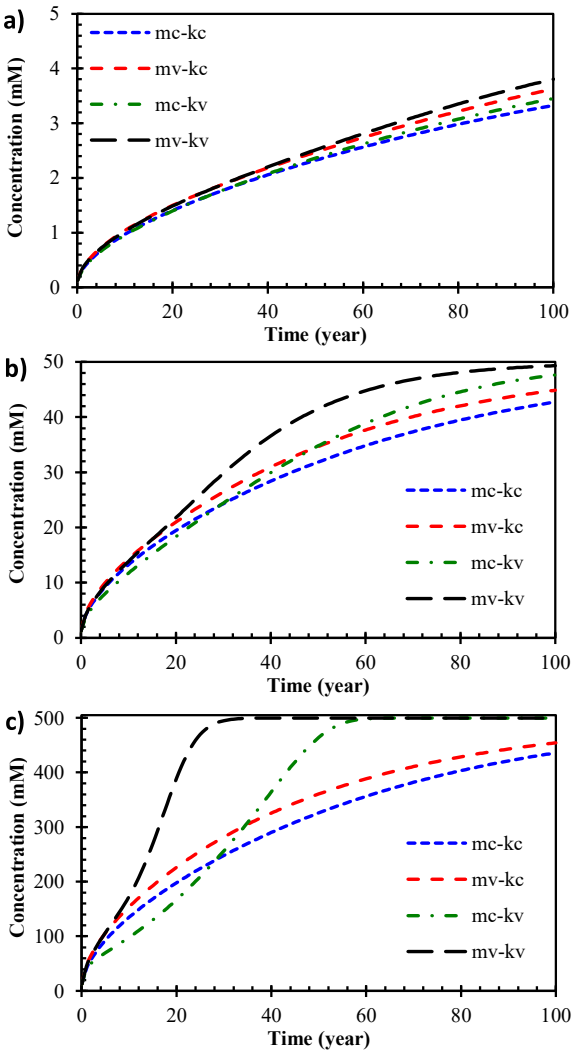

Fig. 10. Breakthrough of average solute concentration in the barrier using a) scenario 1, b) scenario 2, and c) Scenario 3 in Table 4.

Fig. 14(c) shows the breakthrough of the average solute concentration using scenario 10 with the highest hydraulic conductivity among all scenarios. The variable hydraulic conductivity plays a significant role in the solute breakthrough due to the role of Darcian fluid flow convection. Therefore, Fig. 14(c) shows a faster breakthrough of solute concentration when using mc-kv and mv-kv approaches compared with mc-kc and mv-kc approaches. This difference is less considerable in scenario 2 (Fig. 14(b)), where the hydraulic conductivity is less than scenario 10 (Fig. 14(c)).

7. Limitations

Nevertheless, there are still some limitations and simplifications that need to be refined in future studies. First, it was assumed that the soil body is rigid, whereas mechanical consolidation, chemical consolidation, and osmotic consolidation may induce some deformations in the clayey barriers. Mechanical consolidation occurs as a result of surcharging loads of waste and soil layers. Chemical consolidation is induced by chemico-osmotic fluid and negative pore water pressure. Osmotic consolidation also occurs due to the effect of solutes on shrinkage of diffuse double layer and electrostatic repulsive minus attractive stresses [62–64]. Therefore, coupled hydro-chemico-mechanical multiphase flow will actually govern the solute transport in a clayey barrier due to changes in void ratio and its effect on hydraulic conductivity and membrane efficiency. Besides that, the temperature gradient also affects the flow in the porous media, which considering it results in more accurate outcomes [65–67].

This study used 49 and 30 data points on membrane efficiency and apparent tortuosity to develop practical models for them, respectively. Due to the lack of sufficient experimental data points on those parameters, more validation or extension of models was not possible, which can be improved by conducting more experiments and field explorations on these parameters. In addition, the time-consuming procedure of experiments on clays and the dependency of results on material and the apparatus type are a few reasons

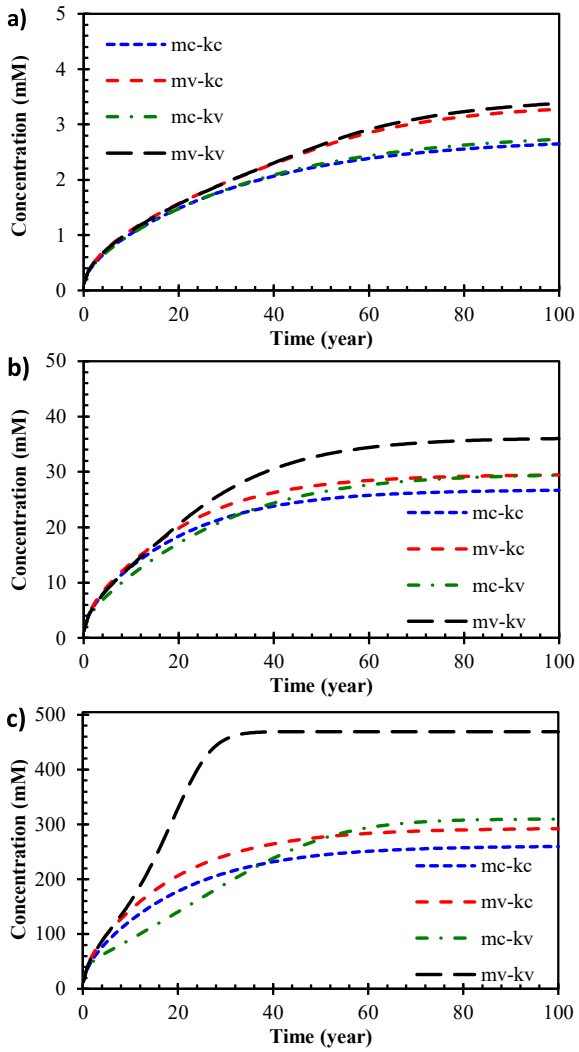

Fig. 11. Breakthrough of average solute concentration in the barrier using a) scenario 4, b) scenario 5, and c) Scenario 6 in Table 4.

for the limited data availability [68].

Additionally, field or laboratory results on the coupled multiphase solute transport in the clayey barriers under controlled conditions are needed to validate the numerical solution provided in this study. However, such data points are not available due to the complexity of the processes, timely transport process in clayey soils, and multiplicity influential factors (i.e., mechanical changes, electrical and thermal gradient) [4].

This study attempted to investigate different conditions by assuming different values for the source solute concentration, exit boundary condition, barrier thickness, and hydraulic gradient in the numerical modelling. Nevertheless, using a different clayey material, soluble contaminant, porosity, adsorption coefficient, Robin, or Cauchy boundary condition at the bottom boundary, and using different values for source solute concentration, barrier thickness, and hydraulic gradient besides what has been used in this study, may result in different results. Moreover, there are some simplifications in the partial differential equation used in this study, such as the assumption of one-dimensional coupled multiphase flow. However, there are some conditions where there are two or three-dimensional coupled flows. For instance, there are undeniable hydraulic and concentration gradients in the horizontal direction close to the boundaries and edges of a clayey barrier.

Furthermore, this study used Na-bentonite material from Malusis and Shackelford's study (2002) [32], while using other materials in the numerical study or developing empirical models may affect outcomes. It is noteworthy that leachate has very complex components including dissolved organic matter, inorganic macro components, heavy metals, xenobiotic organic compounds, etc. [69,70]. Therefore, exploring their effects on clayey barriers and changing their properties need experimental studies at the first step, whose outcomes may be used to improve the accuracy of present numerical studies.

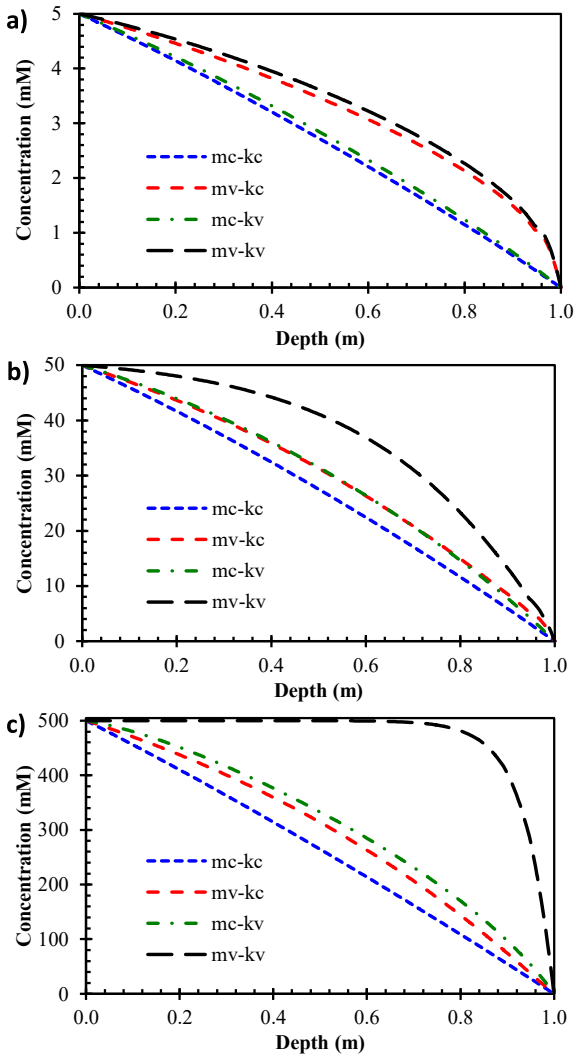

Fig. 12. Solute concentration profile in a) scenario 4, b) scenario 5, and c) Scenario 6 in Table 4 in the 100th year.

8. Conclusions

It has been a constant effort to improve the knowledge about clayey barriers' behavior by conducting experiments, developing analytical equations, and improving the accuracy of numerical models. Malusis et al. (2001) introduced a new apparatus to measure membrane efficiency, which led to more exploration of the membrane behavior of various clays [33]. It also improved the accuracy of numerical models on solute transport by not ignoring membrane efficiency in equations. Comparative results demonstrated the substantial role of membrane behavior in clayey barriers [19,61]. Although it was a significant step, there were still many simplifications.

Most of the previous numerical studies regarding the solute transport and multiphase hydro-chemical flow in a clayey barrier assumed that membrane efficacy, diffusion coefficient, and hydraulic conductivity remain constant during the time. However, due to the continuous changes in solute concentration profile and the concentration-dependent nature of those coefficients, assuming constant coefficients is a considerable simplification. Therefore, this study took another step toward a more accurate numerical modelling of solute transport in a clayey barrier by using concentration-dependent coefficients.

As a first step, a previously published concentration-dependent model of hydraulic conductivity for chemically active clays was adopted. Then, an empirical model for apparent tortuosity and a semi-empirical model for membrane efficiency were developed based on existing experimental data on the Na-bentonite. Finally, this study defined four approaches to apply these coefficients in ten numerical scenarios to prospect the solute transport.

In general, variable hydraulic conductivity is higher than its constant value as solute existence in the pore fluid increases the hydraulic conductivity. In addition, using variable membrane efficiency instead of the constant approach leads to lower membrane efficiency in shallower parts and higher membrane efficiency in deeper parts in the early years, whereas, over the long term, and after

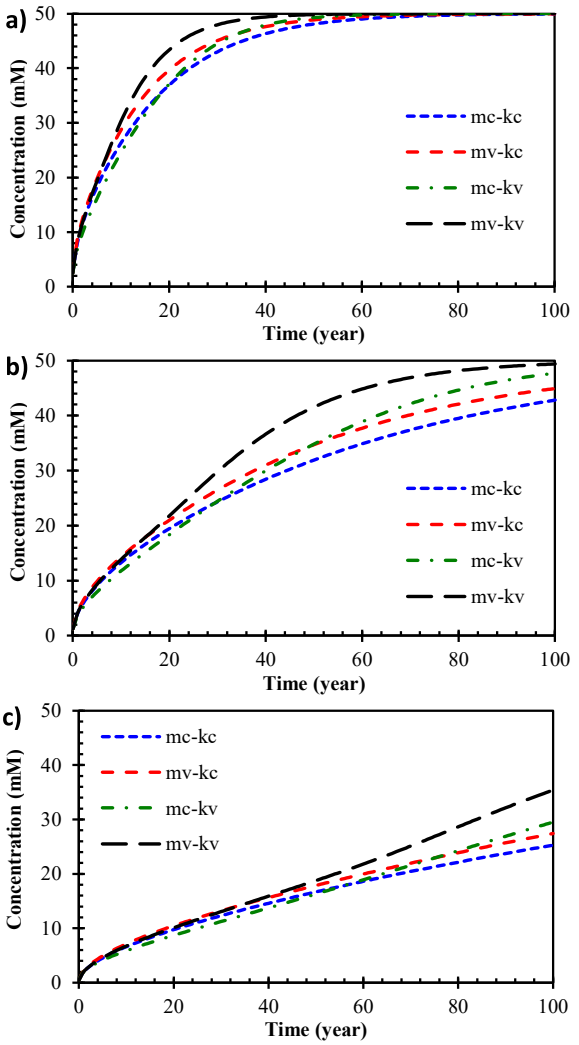

Fig. 13. Breakthrough of average solute concentration in the barrier using a) scenario 7, b) scenario 2, and c) Scenario 8 in Table 4.

solute advancements in deeper parts, the variable approach results in lower membrane efficiency all over the barrier compared with the constant approach.

Using constant hydraulic conductivity to design clayey barriers leads to lower Darcian and chemico-osmosis fluid flow. Choosing the approach to apply hydraulic conductivity becomes more noticeable over time as the solute leakage affects more parts of the barrier. Variable hydraulic conductivity is able to reflect the effect of solute leakage on hydraulic conductivity but not constant hydraulic conductivity. Depending on the barrier's conditions, it may lead to significantly inaccurate predictions on the solute breakthrough in the barrier and groundwater contamination. In addition, using constant membrane efficiency in designing the clayey barrier leads to the inaccurate estimation of solute breakthrough due to overestimated restriction ability in some parts and underestimating that in others. Ten numerical scenarios and four approaches for applying membrane efficiency and hydraulic conductivity were defined to explore the extent of these effects. Results were used to derive engineering applications for designing clayey barriers.

Using variable membrane efficacy instead of the constant value affects the results more significantly in diluted concentrations due to the stronger restriction ability of clays in diluted concentrations. However, using variable hydraulic conductivity changes the result more noticeably in higher concentrations due to the considerable increase of hydraulic conductivity in concentrated areas. Therefore, for the sake of simplicity in engineering applications in diluted concentrations, it is possible to use constant hydraulic conductivity, while assuming the constant membrane efficiency misleads the solute breakthrough prediction significantly, especially in the long term. Although membrane efficiency is negligible in higher concentrations, using constant membrane efficiency for designing purposes is fallacious because the combination of variable hydraulic conductivity and constant membrane efficiency overestimates the inhibitory role of chemico-osmosis convection, which results in predicting slower breakthrough of solutes for designing purposes.

Furthermore, this paper also looked at the effects of the exit boundary condition on the results using various approaches to apply coefficients. In general, using different approaches leads to utterly different steady-state conditions when using $c(L,t) = 0$ as the exit

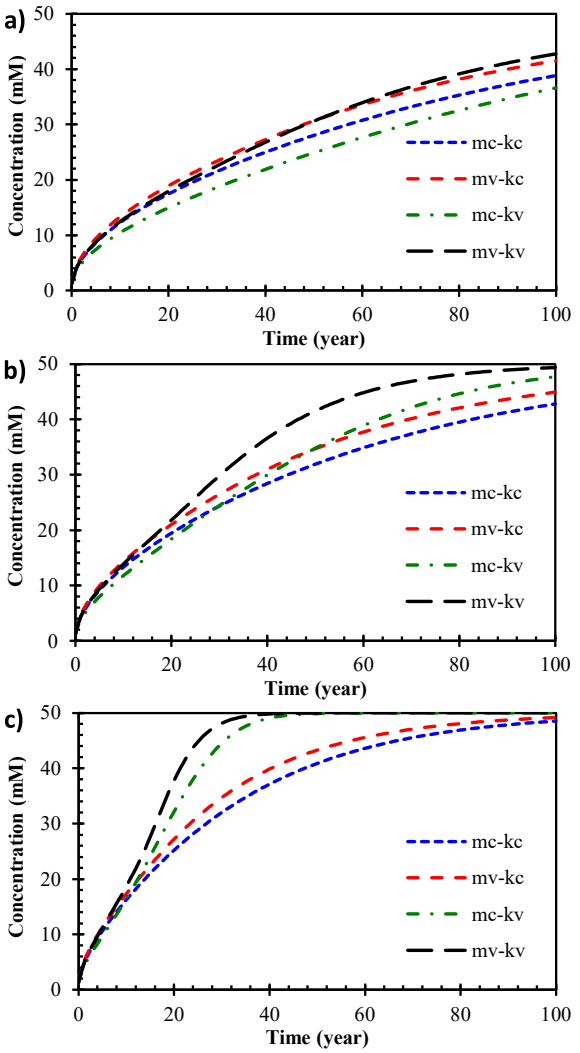

Fig. 14. Breakthrough of average solute concentration in the barrier using a) scenario 9, b) scenario 2, and c) Scenario 10 in Table 4.

boundary condition, whereas the steady-state condition is the same when using $\partial c(L,t)/\partial y = 0$ as the exit boundary condition, and the difference between approaches appears in terms of time to reach the steady-state condition. *Thus, if the barrier is designed based on the steady-state condition or its condition in the very long term, selecting the approach for applying coefficients is not critical when the governing boundary condition is* $\partial c(L,t)/\partial y = 0$. *As a result, for the sake of simplicity, the constant approach can be used in the long term, whereas if a determined time is concerned, using the constant approach is misleading. Nevertheless, when the governing boundary condition is* $c(L,t) = 0$, *assuming the constant approach in the barrier's design leads to underestimating the solute transport rate, which makes it indispensable to use the variable approach for environmental engineering applications.*

Comparing the solute concentration breakthrough in the barriers with various thicknesses demonstrates that the difference between the results of various approaches is negligible and vanishes sooner. For engineering design purposes, thick barriers need to be designed using the variable approach, while thin barriers can be designed using the constant approach.

This study also investigates the effect of hydraulic gradient on the results using different approaches. Results indicate that variable hydraulic conductivity influences chemico-osmosis fluid flow and the inhibitory role of its convection significantly in the low hydraulic gradient. However, in higher hydraulic gradients, Darcian fluid flow and its respective convection affect the solute breakthrough considerably. Thus, variable hydraulic conductivity combined with variable membrane efficiency should be applied in higher hydraulic gradients. Otherwise, the role of convection is underestimated. However, the constant hydraulic conductivity leads to the overestimation of solute transport, which can be applied for the sake of a more conservative design.

Until now, constant membrane efficiency and hydraulic conductivity were assumed to model the contaminant transport and design clayey barriers based on their efficiency to decrease the leakage rate. Exploring the result in various scenarios using different approaches leads to a general conclusion that picking the variable approach for applying membrane efficiency and hydraulic conductivity leads to considerable differences in results. Considering the fact that using concentration-dependent coefficients leads to a higher

rate of contaminants transport in many cases, mainly in the long term, and their concentration-dependent nature confirmed by experimental results, using other approaches may be misleading and ends up in the inaccurate design of barriers, which endanger the health of soil and groundwater.

Author contribution statement

Hamed Sadeghi: Wrote the paper; Analyzed and interpreted the data; Contributed reagents, materials, analysis tools or data.
Aysa Hedayati-Azar: Wrote the paper; Analyzed and interpreted the data.

Data availability statement

The data that support the findings of this study are available on request from the corresponding author

Declaration of interest's statement

The authors declare that they have no known competing financial interests or personal relationships that could have appeared to influence the work reported in this paper.

Acknowledgments

The corresponding author is grateful to the Iran's National Elites Foundation for the financial support provided to him by way of "Dr Kazemi-Ashtiani Award". The financial support provided by Iran National Science Foundation by way of grant 4000730 is also acknowledged.

References

[1] D. Laner, et al., A review of approaches for the long-term management of municipal solid waste landfills, Waste Manag. 32 (3) (2012) 498–512.
[2] C. Shackelford, S. Moore, Fickian diffusion of radionuclides for engineered containment barriers: diffusion coefficients, Porosities, and complicating issues, Eng. Geol. 152 (2013) 133–147.
[3] A. Hedayati-Azar, H. Sadeghi, A review of research approaches to contaminant transport in saturated deformable clay under coupled hydro-chemico-mechanical processes, 3, Sharif J. Mechan. Eng. 37 (2) (2021) 97–115.
[4] C. Shackelford, et al., Research challenges involving coupled flows in geotechnical engineering, Geotechn. Fund. Add. New World Challeng. (2019) 237–274. Springer.
[5] H. Sadeghi, C.W. Ng, Shear behaviour of a desiccated loess with three different microstructures, in: 7th International Conference on Unsaturated Soils, 2018.
[6] H. Sadeghi, A. Kolahdooz, M.-M. Ahmadi, Slope stability of an unsaturated embankment with and without natural pore water salinity subjected to rainfall infiltration, Rock Soil Mech. 43 (8) (2022) 2136.
[7] M. Manassero, in: On the Fabric and State Parameters of Active Clays for Contaminant Control, Proceedings of the 19th International Conference of Soil Mechanics and Geotechnical Engineering, Seoul, Korea, 2017.
[8] M.A. Malusis, C.D. Shackelford, H.W. Olsen, Flow and transport through clay membrane barriers, Eng. Geol. 70 (3–4) (2003) 235–248.
[9] M. Manassero, The second ISSMGE Kerry Rowe Lecture: on the intrinsic, state and fabric parameters of active clays for contaminant control, Can. Geotech. J. 57 (2019).
[10] C. Teng, et al., Characterization and Treatment of Landfill Leachate: A Review, vol. 203, Water research, 2021, 117525.
[11] A. Kolahdooz, H. Sadeghi, M.M. Ahmadi, A numerical study on the effect of salinity on stability of an unsaturated railway embankment under rainfall, in: E3S Web of Conferences, EDP Sciences, 2020.
[12] J. Mitchell, Conduction phenomena: from theory to geotechnical practice, Geotechnique 41 (3) (1991) 299–340.
[13] M.A. Malusis, C.D. Shackelford, Chemico-osmotic efficiency of a geosynthetic clay liner, J. Geotech. Geoenviron. Eng. 128 (2) (2002) 97–106.
[14] J.-B. Kang, C.D. Shackelford, Clay membrane testing using a flexible-wall cell under closed-system boundary conditions, Appl. Clay Sci. 44 (1–2) (2009) 43–58.
[15] N. Shariatmadari, M. Salami, M. Karimipour fard, Effect of inorganic salt solutions on some geotechnical properties of soil-bentonite mixtures as barriers, Int. J. Civ. Eng. 9 (2) (2011) 103–110.
[16] A.K. Mishra, et al., Controlling factors of the swelling of various bentonites and their correlations with the hydraulic conductivity of soil-bentonite mixtures, Appl. Clay Sci. 52 (1–2) (2011) 78–84.
[17] Z. Zhang, G. Tian, L. Han, Influence of chemical osmosis on solute transport and fluid velocity in clay soils, Open Chem. J. 18 (1) (2020) 232–238.
[18] Z. Zhang, et al., Modeling fully coupled hydraulic-mechanical-chemical processes in a natural clay liner under mechanical and chemico-osmotic consolidation, Environ. Sci. Pollut. Control Ser. 25 (36) (2018) 36173–36183.
[19] M. Manassero, A. Dominijanni, Modelling the osmosis effect on solute migration through porous media, Geotechnique 53 (5) (2003) 481–492.
[20] M.A. Malusis, C.D. Shackelford, Explicit and implicit coupling during solute transport through clay membrane barriers, J. Contam. Hydrol. 72 (1–4) (2004) 259–285.
[21] S. Bader, H. Kooi, Modelling of solute and water transport in semi-permeable clay membranes: comparison with experiments, Adv. Water Resour. 28 (3) (2005) 203–214.
[22] S.P. Neuman, Theoretical derivation of Darcy's law, Acta Mech. 25 (3) (1977) 153–170.
[23] A. Bazargan, et al., An unsteady state retention model for fluid desorption from sorbents, J. Colloid Interface Sci. 450 (2015) 127–134.
[24] H. Sadeghi, P. AliPanahi, Saturated hydraulic conductivity of problematic soils measured by a newly developed low-compliance triaxial permeameter, Eng. Geol. 278 (2020), 105827.
[25] S.J. Fritz, Ideality of clay membranes in osmotic processes: a review, Clay Clay Miner. 34 (2) (1986) 214–223.
[26] C.J. Lynde, Osmosis in soils: soils act as semi-permeable membranes, Agron. J. 4 (1) (1912) 102.
[27] A. Dominijanni, M. Manassero, Modelling the swelling and osmotic properties of clay soils. Part I: the phenomenological approach, Int. J. Eng. Sci. 51 (2012) 32–50.
[28] A. Dominijanni, M. Manassero, Modelling the swelling and osmotic properties of clay soils. Part II: the physical approach, Int. J. Eng. Sci. 51 (2012) 51–73.
[29] M.H. Gleason, D.E. Daniel, G.R. Eykholt, Calcium and sodium bentonite for hydraulic containment applications, J. Geotech. Geoenviron. Eng. 123 (5) (1997) 438–445.

[30] A. Hedayati-Azar, H. Sadeghi, Semi-empirical modelling of hydraulic conductivity of clayey soils exposed to deionized and saline environments, J. Contam. Hydrol. (2022), 104042.
[31] C. Shackelford, Membrane behavior in engineered bentonite-based containment barriers: state of the art, Coupled phenomena in environmental geotechnics (2013) 45–60.
[32] M.A. Malusis, C.D. Shackelford, Theory for reactive solute transport through clay membrane barriers, J. Contam. Hydrol. 59 (3–4) (2002) 291–316.
[33] M.A. Malusis, C.D. Shackelford, H.W. Olsen, A laboratory apparatus to measure chemico-osmotic efficiency coefficients for clay soils, Geotech. Test J. 24 (3) (2001) 229–242.
[34] G.L. Bohnhoff, K.M. Sample-Lord, C.D. Shackelford, in: Geo-Chicago (Ed.), Advances in the Membrane Behavior of Bentonite-Based Barriers vol. 2016, 2016, pp. 329–338.
[35] C.D. Shackelford, D.E. Daniel, Diffusion in saturated soil. I: background, J. Geotechn. Eng. 117 (3) (1991) 467–484.
[36] W. Stępniewski, H. Sobczuk, M. Widomski, Diffusion in soils, in: Encyclopedia of Agrophysics, Springer Netherlands, 2011, pp. 214–220.
[37] C.D. Shackelford, Diffusion of Inorganic Chemical Wastes in Compacted Clay, Texas Univ., Austin, TX (USA), 1989.
[38] C.D. Shackelford, Diffusion of Contaminants through Waste Containment Barriers, Transportation Research Record, 1989, p. 1219.
[39] M.A. Malusis, J.-B. Kang, C.D. Shackelford, Restricted salt diffusion in a geosynthetic clay liner, Environ. Geotechn. 2 (2) (2015) 68–77.
[40] J.-g. Liu, H.-t. Wang, Y.-f. Nie, Fractal model for predicting effective diffusion coefficient of solute in porous media, Adv. Water Sci. 15 (4) (2004) 458–462.
[41] A. Meier, et al., in: Persistence of Semipermeable Membrane Behavior for a Geosynthetic Clay Liner, Proceedings, 7th International Conference on Environmental Geotechnics, Melbourne, Australia, 2014.
[42] C.D. Shackelford, A. Meier, K. Sample-Lord, Limiting membrane and diffusion behavior of a geosynthetic clay liner, Geotext. Geomembranes 44 (5) (2016) 707–718.
[43] A. Dominijanni, M. Manassero, in: Modelling Advective, Diffusive and Osmotic Transport with Reference to the Molecular Scale, Geotechnical problems with man-made and man influenced grounds, Prague, Czech Republic, 2003, pp. 327–332.
[44] J.-B. Kang, C.D. Shackelford, Consolidation enhanced membrane behavior of a geosynthetic clay liner, Geotext. Geomembranes 29 (6) (2011) 544–556.
[45] A.K. Mishra, et al., Effect of salt concentrations on the hydraulic conductivity of the mixtures of basalt soil and various bentonites, J. Facul. Agr. 51 (1) (2006) 37–43.
[46] M.Y. Weimin, et al., Effects of salt solutions on the hydro-mechanical behavior of compacted GMZ01 bentonite, Environ. Earth Sci. 72 (7) (2014) 2621–2630.
[47] J. Dutta, A. Mishra, A study on the influence of inorganic salts on the behaviour of compacted bentonites, Appl. Clay Sci. 116–117 (2015) 85–92.
[48] R.P. Chapuis, Predicting the saturated hydraulic conductivity of soils: a review, Bull. Eng. Geol. Environ. 71 (3) (2012) 401–434.
[49] M. Mbonimpa, et al., Practical pedotransfer functions for estimating the saturated hydraulic conductivity, Geotech. Geol. Eng. 20 (3) (2002) 235–259.
[50] M. Wyllie, G. Gardner, The generalized kozeny-carman equation, World Oil 146 (4) (1958) 121–128.
[51] M. Wyllie, G. Gardner, The generalized kozeny-carman equation, World Oil 146 (5) (1958) 210–228.
[52] K.M. Sample-Lord, et al., Apparent salt diffusion coefficients for soil–bentonite backfills, Can. Geotech. J. 57 (5) (2020) 623–634.
[53] H. Sadeghi, et al., Geotechnical characterization and collapsibility of a natural dispersive loess, Eng. Geol. 250 (2019) 89–100.
[54] J.-B. Kang, C.D. Shackelford, Membrane behavior of compacted clay liners, J. Geotech. Geoenviron. Eng. 136 (10) (2010) 1368–1382.
[55] Q. Tang, et al., Membrane behavior of bentonite-amended compacted clay, Soils Found. 54 (3) (2014) 329–344.
[56] Q. Tang, et al., Geo-characterization and Modeling for Sustainability, 2014, in: Influence of Compaction Degree on Membrane Behavior of Compacted Clay Amended with Bentonite, Geo-Congress, 2014.
[57] M.A. Malusis, Membrane Behavior and Coupled Solute Transport through a Geosynthetic Clay Liner, Colorado State University, 2001.
[58] Z. Zhang, L. Han, M. Wang, Influence of variable membrane behavior of clay on solute transport, Environ. Eng. Sci. 38 (11) (2021) 1087–1097.
[59] A. Comsol, COMSOL Multiphysics Reference Manual, 2007.
[60] H. Sadeghi, et al., A vacuum-refilled tensiometer for deep monitoring of in-situ pore water pressure, Sci. Iran. 27 (2) (2020) 596–606.
[61] M.A. Malusis, C.D. Shackelford, Coupling effects during steady-state solute diffusion through a semipermeable clay membrane, Environ. Sci. Technol. 36 (6) (2002) 1312–1319.
[62] S. Barbour, D. Fredlund, Mechanisms of osmotic flow and volume change in clay soils, Can. Geotech. J. 26 (4) (1989) 551–562.
[63] H. Sadeghi, H. Nasiri, Hysteresis of soil water retention and shrinkage behaviour for various salt concentrations, Géotech. Lett. 11 (1) (2021) 1–9.
[64] M. Kaczmarek, T. Hueckel, Chemo-mechanical consolidation of clays: analytical solutions for a linearized one-dimensional problem, Transport Porous Media 32 (1) (1998) 49–74.
[65] S. Olivella, et al., Porosity variations in saline media caused by temperature gradients coupled to multiphase flow and dissolution/precipitation, Transport Porous Media 25 (1) (1996) 1–25.
[66] A.J. Landman, R.J. Schotting, Heat and brine transport in porous media: the Oberbeck-Boussinesq approximation revisited, Transport Porous Media 70 (3) (2007) 355–373.
[67] S. Olivella, et al., Nonisothermal multiphase flow of brine and gas through saline media, Transport Porous Media 15 (3) (1994) 271–293.
[68] C. Shackelford, J. Scalia, Semipermeable membrane behavior in bentonite-based barriers: past, present, and future, in: Proceed. GeoVancouver, 2016.
[69] P. Kjeldsen, et al., Present and long-term composition of MSW landfill leachate: a review, Crit. Rev. Environ. Sci. Technol. 32 (4) (2002) 297–336.
[70] N. Mokni, et al., Deformation and flow driven by osmotic processes in porous materials: application to bituminised waste materials, Transport Porous Media 86 (2) (2011) 635–662.